KFUPM
Journal of Undergraduate Research International

Diamond Open Access 88

Article Geosciences

Optimizing Mineral Exploration Workflows: A Quantitative Evaluation of the Agreement Between Handheld and Laboratory Geochemical and Petrophysical Instruments

Farah Abdullah Alajmi and Muhammad Hammad Malik*

Cite https://doi.org/10.64589/juri/231589

Submitted: April 24, 2026 **Revised:** May 04, 2026 **Accepted:** May 10, 2026

ABSTRACT

The criticality of portable analytical tools has gained traction with an increasing trend in mineral exploration projects globally. Handheld instruments have become integral to the rapid and efficient collection of geochemical and petrophysical data from field environments for such mineral exploration workflows. However, reservations regarding the results are exist. Although handheld instruments are faster, cheaper, and denser than laboratory-based techniques, concerns remain regarding their analytical reliability. Herein, we evaluated the concordance between several handheld and laboratory measurements by analyzing eight various homogeneous (pure minerals) and heterogeneous rock samples. The instruments used in our study included portable X-ray fluorescence (pXRF), laboratory-based XRF, and X-ray diffraction, portable permeability instrument TinyPerm 3, and conventional laboratory porosity measurement methods. Several simple statistical tools were used to compare the results. Although handheld tools work well for quick screening and spatial geochemical mapping of major minerals, they are not extremely accurate for minute details, particularly in the case of trace elements. However, these differences between handheld and laboratory results can also arise because of simple and common analytical issues, such as sample preparation, surface roughness, matrix effects, and detection limits. Therefore, the use of a hybrid analytical workflow that combines portable measurements with targeted selected samples for laboratory validation is suggested to make exploration more efficient while keeping the data reliable.

Keywords: permeability measurement, helium porosimeter, X-ray fluorescence spectroscopy, X-ray diffraction analysis, AxioScan

1. INTRODUCTION

With technological advancements, handheld analytical instruments are widely utilized in multiple aspects of geology, particularly in mineral exploration. Several handheld tools, such as portable X-ray fluorescence (pXRF) analyzers, portable gamma ray tools, porosity meters, and other handheld petrophysical devices, have helped geologists collect data directly in the field without waiting for lengthy and time-consuming laboratory findings. This advancement in technology has facilitated fieldwork faster, more efficient, and relatively precise, especially in early exploration stages, where quick decisions can play crucial roles [1,2] Compared to complicated and relatively expensive laboratory techniques such as X-ray diffraction (XRD), X-ray fluorescence (XRF), or helium porosimetry, these handheld instruments generally require minimal to no sample preparation while providing immediate results. Considering this advantage, they are now being increasingly employed for screening mineral samples, identifying major lithologies, and guiding further sampling strategies for mineralogical studies in mineral exploration campaigns.

However, although handheld instruments and their swift results are convenient, their accuracy and reliability are still debated among researchers. Although these portable devices are based on scientific principles similar to laboratory instruments, major differences in their design and performance exist. For instance, portable XRF (pXRF) devices typically require lower power and simpler calibration than laboratory XRF systems, which usually require high-voltage inputs and better detection limits. Such analytical differences can affect their ability to accurately measure certain elements, particularly lighter elements or elements that are present in extremely small or trace amounts, such as rare earth elements[2]. Consequently, the quality of the results gathered from handheld instruments is often dependent on the instrument itself and sample type being investigated.

Another major factor influencing handheld measurements is the selection of the sample to be analyzed. When samples are crushed into a powder and properly prepared, even handheld instruments can produce results that are much closer to those obtained from laboratory analyses[3]. However, when measurements are directly performed on rough rock surfaces, the findings tend to be less consistent. This was primarily due to the presence of uneven surfaces, small cracks and fractures, and variations in the mineral composition across the sample. Similar results were reported by other authors too[4]. They found that powdered

Published under an exclusive license by KFUPM

samples provided more reliable results than unprepared drill cores, underscoring the criticality of proper sample handling. Another crucial concern is the effect of the sample composition and heterogeneity, often referred to in the literature as matrix effects. Different minerals present in rock formations can affect the absorption or emission of X-rays, resulting in errors in measured values [1]. Additionally, other factors such as the presence of moisture, surface roughness, and weathering contamination can influence readings. Even small differences in sample preparation can lead to noticeable alterations in measurements [5]. These findings highlight the criticality of following consistent procedures when using handheld instruments.

Similar challenges are noted when handheld petrophysical tools are employed to measure properties such as porosity and permeability. Although these devices are useful for quick field estimates, they often measure only a small sample portion and may not represent all rock properties. However, laboratory methods for porosity and permeability analyses typically involve more controlled conditions and provide more accurate findings. Although handheld devices can provide useful estimates, significant differences can exist compared to laboratory measurements, particularly in rocks that do not have a uniform composition [2,6]. Considering these limitations, several researchers have suggested using handheld instruments as part of a combined approach rather than as a complete replacement for laboratory analyses. In this approach, handheld tools are utilized for quick screening and patterns identification, whereas laboratory methods are utilized to confirm important finings. A proper workflow using a pXRF instrument in the field to guide sampling strategies, with selected samples subsequently examined in the laboratory for enhanced data control was also described by other researchers [7]. This approach is believed to save time and cost while maintaining the quality of the data acquired.

Overall, handheld instruments provide clear advantages in terms of analysis speed and convenience, particularly in the modern mineral exploration environment. They are especially useful for the initial screening of samples, the identification of detectable trends, and making quick decisions in the field. However, the limitations of such instruments must be considered, particularly when higher accuracy is necessary. Although portable instruments cannot completely replace sophisticated laboratory analyses, they play a crucial role when used correctly and alongside proper quality control.

Although several studies have investigated these portable tools, few have conducted geochemical and petrophysical measurements across different rock types, including mineralogically homogeneous and heterogeneous rocks. Additionally, some studies rely solely on correlation without completely analyzing the differences between methods. Our study aimed to address these gaps by comparing handheld and laboratory results using a more detailed statistical approach. We attempted to establish confidence in use of the handheld instruments for routine geological and mineral exploration studies by evaluating their reliability for routine geological and mineral exploration.

2. MATERIALS & METHODOLOGY APPLIED

2.1. Materials. The materials utilized in this study consisted of rock samples locally sourced from different regions of the Kingdom of Saudi Arabia. Table 1 lists the details of the samples. These samples include F1, an igneous rock (Precambrian-aged granite) sourced from the Midyan region of NW Saudi Arabia, and two carbonate rock samples (F2 and F8) of Miocene age (approximately 15 Ma) sourced from the eastern region of the Kingdom, including one (F8) from the outcrops exposed in King Fahd University of Petroleum and Minerals (KFUPM). Two sandstone samples (F4 and F5) were included, one of Cambrian age (530 Ma) sourced from the AlUla region and another of Permian age (approximately 290 Ma) sourced from the Qasim Region. Furthermore, the samples included one anhydrite (F6) and one dolomite (F7) rock sample of Permian age (250 Ma) sourced from the Qasim Region of Saudi Arabia.

These samples were first tested using portable equipment for the initial data, and later subjected to sample preparation and detailed laboratory analysis using in-house equipment at the Center for Integrative Petroleum Research (CIPR) at KFUPM.

3. METHODOLOGY APPLIED

3.1. Handheld Analysis.

(a) TinyPerm 3: Portable handheld air permeability measurement instrument TinyPerm©3 (manufactured by New England Research, USA) was used for permeability measurements (Fig 1). This instrument is a portable air permeameter and is utilized to measure matrix permeability and effective fracture apertures at the outcrop in the field and at core samples in laboratories [8,9]. The instrument operation is based on the transient pressure decay principle and consists of a rubber nozzle that is pressed against the rock surface, forming airtight contact. A pulse of compressed air is initially manually pushed into the rock via the instrument pump. As the air is withdrawn, the temporary vacuum pulse generated at the sample is monitored using a microcontroller attached to the instrument. The drop in the resultant pressure is recorded and illustrated in a real-time graph on NER-supplied Android^{TM} mobile phone-based software wirelessly linked to the device via Bluetooth [8]. Particular attention and care are exercised to avoid visibly changed or fractured surfaces in the analysis, because the TinyPerm technique is inherently sensitive to surface conditions. Rough or weathered surfaces may prevent the proper sealing of the probe, resulting in measurement errors. The permeability (k) is calculated from the pressure-decay curve using calibration relationships derived from known standards. This technique assumes a laminar flow through the pore network and is influenced by the pore space connectivity and size near the surface [6].

(b) pXRF Tool: A pXRF tool Tracer 5 XRF Spectrometer (Bruker) was used for the handheld measurements of the constituent elements and minerals (Fig 2). This handheld equipment is a non-destructive device that uses a 50 kV, 4 W Rh target X-ray source on a measurement area of 3–8 mm. A large active area of 20 mm^2 and graphene window of silicon drift detectors (SDD) are used for the detection. Additionally, it has a 1 μm Graphene window to detect lighter elements; however, the usual detection range is from Sodium to Uranium. The working principle is simple, with an X-ray source bombarding the sample with X-rays, which knock electrons from the inner shells of the elements. To fill the vacancy, electrons from the outer shells rush

Table 1. *Descriptive details of the rock samples*

No	Sample	Age	Name	Formation name & Region
1	Granite	Precambrian	F1	Atiyah Monzogranite, Midyan, NW KSA
2	Carbonate	Miocene	F2	Dam Formation, Eastern Province, KSA
3	Gypsum	Permian	F3	Khuff Formation, Qassim Region, KSA
4	Sandstone	Cambrian	F4	Siq Formation, AlUla Region, Western KSA
5	Sandstone	Permian	F5	Unayzah Formation, Qassim Region, KSA
6	Anhydrite	Permian	F6	Khuff Formation, Qassim Region, KSA
7	Dolomite	Permian	F7	Khuff Formation, Qassim Region, KSA
8	Carbonate	Miocene	F8	Umm Rus Formation, KFUPM



Figure 1. TinyPerm 3

to the inner shells and lose binding energy, which is equal to the distance and spacing between two electron shells and is a characteristic of each element[10–12]. The fluorescent detector within the instrument detected the fluorescent energies and were subsequently analyzed. The results are shown in the form of elements and oxide phases in percentages and are displayed on the instrument screen, which can then be uploaded to any computer via a cable.

(c) Handheld Gamma Ray Tool: A handheld Gamma Ray Spectrometer tool (GRS-2000, Gf Instruments) was utilized to detect radioactive elements such as Uranium, Thorium & Potassium (U, Th, and K) in the samples (Fig 3). The instrument is based on a non-destructive, passive measurement method that measures radioactive mineral concentration percentages for K and parts per million (ppm) for U and Th[13,14]. The measurements are conducted by placing the instrument on the rock outcrops/broken samples, and recordings are performed at different time intervals. In this study, a standardized time of 300 s was utilized for the better detection of radioactive elements in the samples. The results

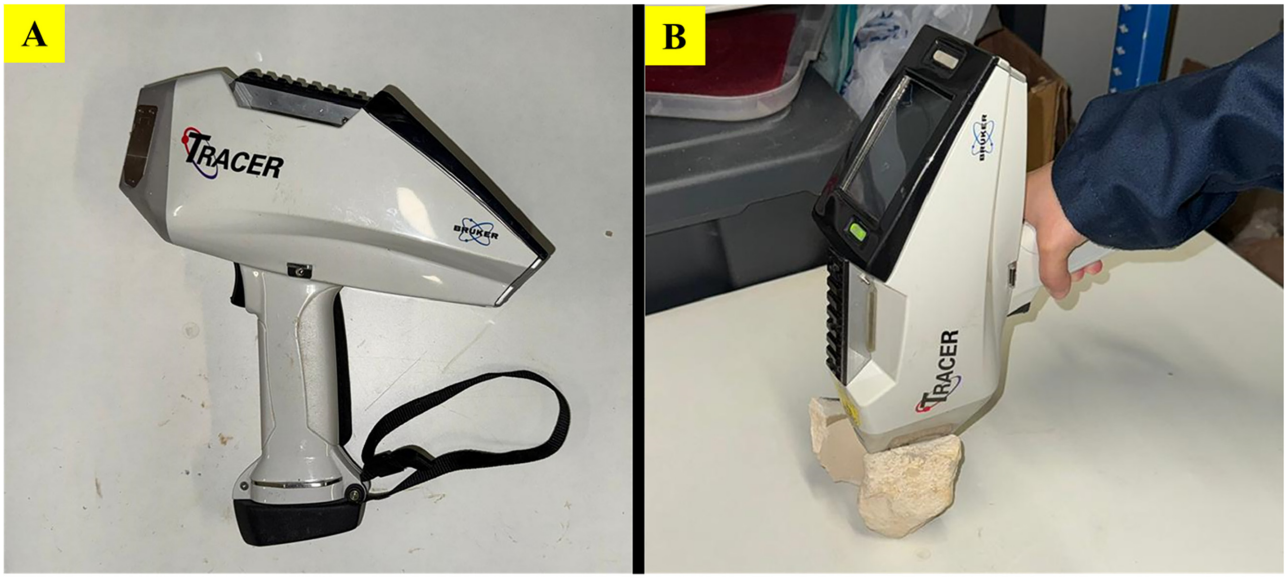

Figure 2. (a) Portable X-ray fluorescence (pXRF) device. (b) pXRF in use

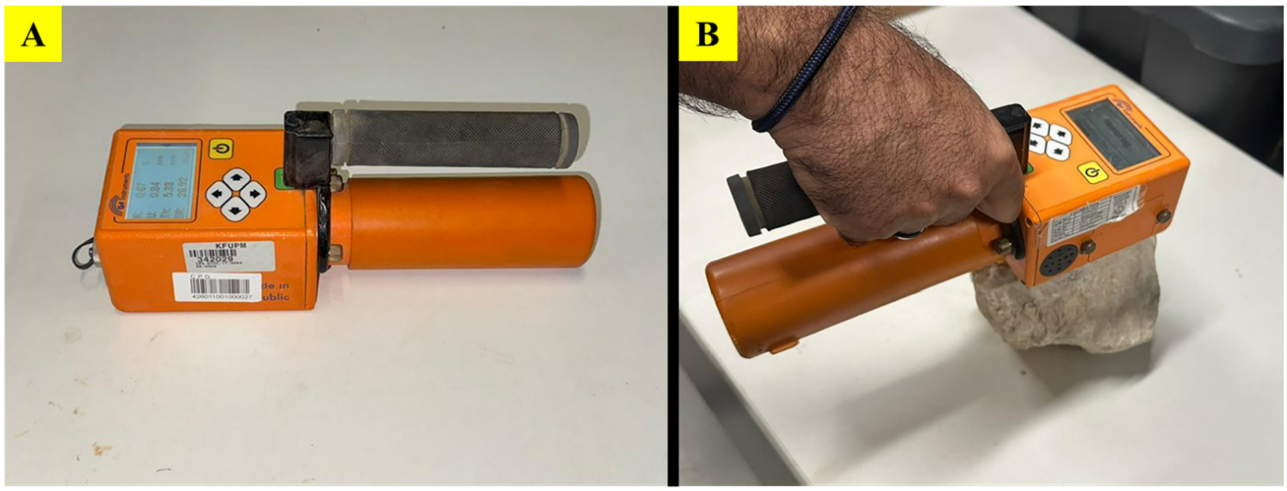

Figure 3. (a) Gamma ray spectrometer tool with F4 results on screen. (b) Tool in use

are directly shown on a screen and exported to computers via data cables.

3.2. Laboratory Analysis. For a detailed laboratory analysis of the samples, high-quality facilities at the CIPR of KFUPM were used. All equipment used in this study were available and operated in-house by highly qualified research scientists at KFUPM.

(d) Petrographic analysis and Point Counting: For petrographic analysis, representative samples were prepared as thin slabs in-house, from which unpolished thin sections with a thickness of approximately 35 µm were produced. These sections were impregnated with blue-dyed resin to help in the identification of pores and estimation of visual porosity permeability using various optical microscopy methods. The prepared thin sections were assessed using an Olympus BX53F petrographic microscope for porosity-permeability estimation using the conventional standard point counting method. The method involves counting standard 300 points using Gazzi–Dickinson's method for each sample to show quantitative data on the inherent mineral composition and porosity[9,15].

(e) Axio Scan: The thin sections were subsequently further scanned using a ZEISS Axio Scan Z1 system, which can simultaneously accommodate up to 20 samples and is operated using ZEN Blue[9,16]. The resulting high-resolution digital images provided an efficient alternative to conventional optical microscopy for thin-section analysis (Fig 4) and were utilized for software-based point counting measurements using JMicrovision v1.3.5.

(f) Quantitative Evaluation of Minerals by Scanning Electron Microscopy: The mineralogical distribution within the samples was determined by automated QEMSCAN. Unpolished thin sections were first carbon-coated using a Q150T Quorum EMS 150R ES system, then examined with an automated QEMSCAN®650F system. The QEMSCAN 650F equipment employed a Quanta 650 FEG scanning electron microscope coupled with a Bruker XFlash energy-dispersive X-ray spectrometer to conduct quantitative mineralogical mapping[9,16]. The data were acquired using an X-ray beam produced at an accelerating voltage of 15 kV and a sample current of 10 nA[17]. The data were subsequently processed using software packages such as iMeasure and iDiscover and presented as color-coded images with various colors representing different minerals and pore spaces (Fig 6).

(g) Laboratory XRF and XRD analysis: For detailed elemental and mineralogical assessments of the samples, XRF and XRD methods were used with high-tech laboratory-based instrumentation. For sample preparation, rock samples were initially pulverized in 4 g dry batches using a Retsch RM 200 mill. Thorough care was taken to minimize contamination by cleaning the equipment with ethanol before and after each run. The powders were subsequently utilized for XRF and XRF analyses.

For elemental characterization, XRF analyses of the pulverized samples were performed using a Bruker AXS Esprit M4 Tornado µXRF system. The instrument used polycapillary lenses to focus the X-ray beam, with detection achieved using the Bruker XFlash SDD[16,18,19].

Mineralogical quantification using XRD analyses were conducted using a Malvern PANalytical Empyrean Cu LFF HR diffractometer operating with Cu Kα_1 radiation at a 1.54060 Å wavelength. The X-ray tube operated at 40 mA and 45 kV, with measurements conducted over a 2θ range of 4–70°[15]. Powders of the samples are mounted on holders and were scanned in the machine at 2 θ positions ranging between 4 and 63°with a scanning time of 8.67 s. The results were subsequently processed using the search-match-module Highscore Plus (v.4.9) with the existing mineralogical archive of ICDD PDF-42022 and exported as charts and tables[15].

4. RESULTS AND STATISTICAL ANALYSIS

4.1. Geochemical Results.

4.1.1. XRF results. The results for all eight samples taken using various equipment are listed in table forms below. The first two tables (Tables 2 and 3) have the elemental results obtained from the samples using handheld and laboratory XRF equipment, respectively. Only a few were detected by handheld XRF, although most transition metals and trace elements were detected by laboratory XRF equipment. Considering this limitation, only major 10 elements encountered in all samples up to the milli-percent level were selected for presentation. These elements represented the bulk composition of the samples.



Figure 4. ZEISS Axio Scan set up

Table 2. *Handheld X-Ray florescence results (%)*

ID	Rock	Ca	Mg	Si	Al	S	Fe	K	Ti	Cr	Mn
F1	Granite	0.29	0.00	75.33	15.01	0.01	0.52	5.29	0.32	0.00	0.01
F2	Carbonate	20.25	33.91	1.27	0.50	0.56	0.23	0.99	0.00	0.00	0.03
F3	Gypsum	20.13	1.82	0.77	0.94	37.78	0.03	0.02	0.00	0.00	0.00
F4	Sandstone	0.15	0.53	65.82	9.29	0.00	1.02	0.04	0.13	0.00	0.01
F5	Sandstone	0.46	0.47	71.40	7.92	0.82	0.29	0.04	0.06	0.00	0.00
F6	Anhydrite	20.42	0.00	0.90	0.93	39.74	0.06	0.03	0.00	0.00	0.00
F7	Carbonate	22.60	52.56	1.96	1.27	0.04	0.29	0.14	0.00	0.00	0.03
F8	Carbonate	22.86	54.13	2.22	0.72	0.06	0.04	0.14	0.00	0.00	0.01

The elemental distribution noted in the samples is presented using pie charts for better visualization (Fig 5). For the first sample (F1), which is an igneous rock, both instruments recorded similar elemental concentrations, raising our hope of greater accuracy for both instruments. The major constituent silica (Si) composition almost matched, whereas the potassium (K) found in feldspars along with Fe was more pronounced in the handheld results than in the laboratory-based results. Alumina (Al) concentrations almost doubled in the lab-based results. The concentrations of other minor elements revealed similar trends. The second group of samples consisted of sandstones represented by F4 and F5, which revealed an almost identical trend. The laboratory-based results exhibited higher concentrations of major elements (Si and Al) in sample F4, whereas for F5, the trend was similar

Table 3. *Laboratory X-Ray florescence results (%)*

ID	Rock Type	Ca	Mg	Si	Al	S	Fe	K	Ti	Cr	Mn
F1	Granite	1.48	0.04	74.19	7.65	0.03	1.92	9.97	0.48	0.05	0.12
F2	Carbonate	76.40	19.41	0.73	0.54	0.20	1.68	0.14	0.15	0.00	0.19
F3	Gypsum	60.15	1.59	0.31	0.37	34.34	1.83	0.04	0.02	0.00	0.02
F4	Sandstone	0.47	0.00	75.34	13.85	0.10	7.81	0.26	0.68	0.02	0.24
F5	Sandstone	1.14	0.00	91.62	2.13	0.44	3.06	0.12	0.31	0.00	0.07
F6	Anhydrite	59.05	0.03	0.19	0.30	39.60	0.46	0.02	0.01	0.00	0.00
F7	Carbonate	76.16	19.35	0.80	0.55	0.07	2.17	0.15	0.06	0.00	0.25
F8	Carbonate	76.61	19.78	1.06	0.76	0.08	0.48	0.27	0.21	0.02	0.05

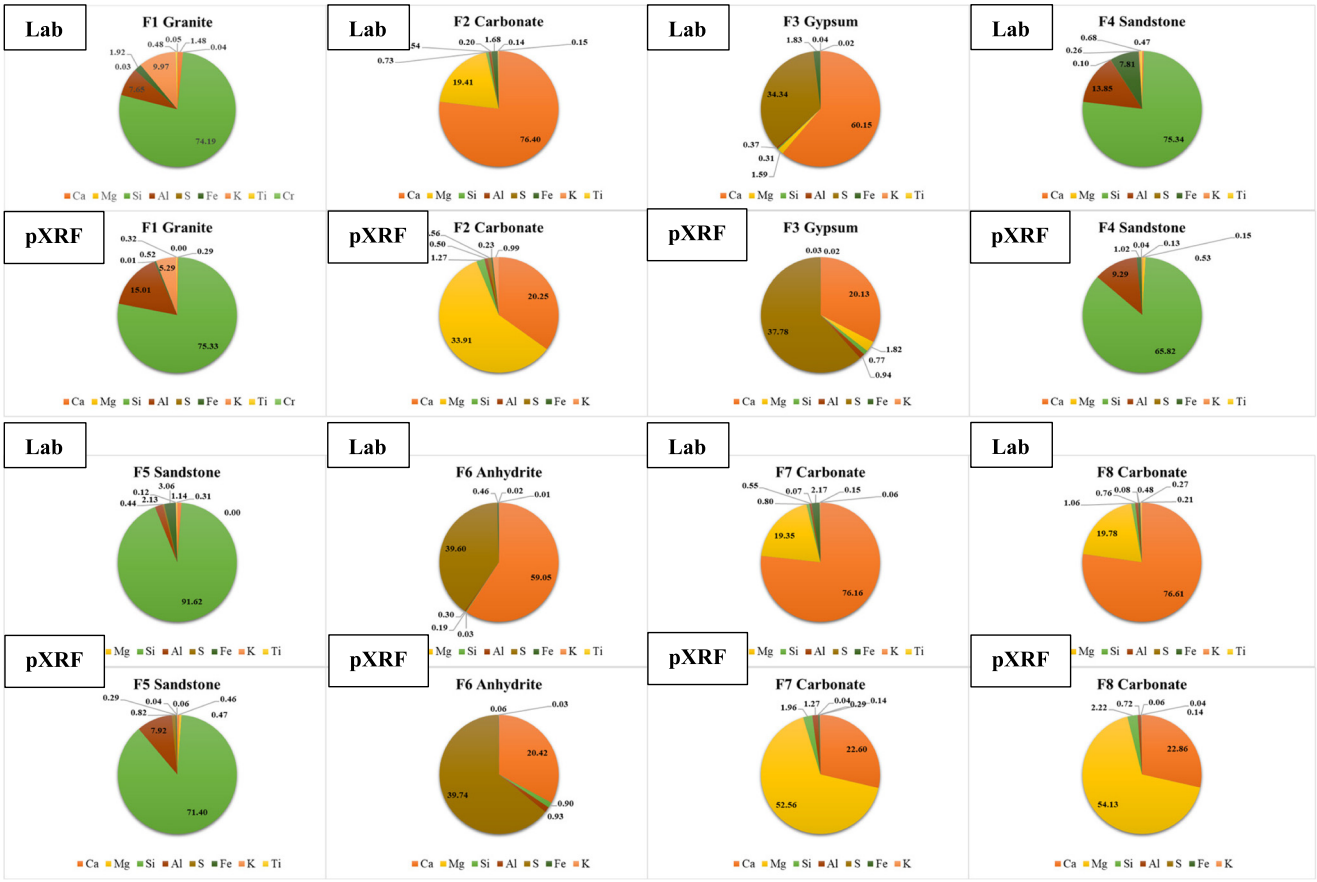

Figure 5. Pie charts based on the lab-based XRD (upper) and handheld XRF findings (lower)

for Si but opposite for Al, which was underrepresented in the laboratory results.

The third group of samples was carbonated and is represented by F2, F7, and F8. The results for carbonates were extremely divergent. Different concentrations of Calcium (Ca) and Magnesium (Mg), which represent the major elements in the carbonates, were noted. In the laboratory results, higher Ca concentrations (>76%) were noted in all samples, whereas Mg concentrations were always <20%. Contrastingly, the handheld results revealed a completely opposite trend, with lower Ca concentrations (<23%) and higher Mg (approximately 50%) concentrations. Possible reasons for this opposite trend are discussed in the Discussion section. Similarly, higher Ca concentrations in the laboratory results and lower concentrations in the handheld results were observed for the gypsum (F3) and anhydrite (F6) samples. Both are calcium rich sulfate ($CaSO_4.2H_2O$, $CaSO_4$) minerals with almost identical S content noted in both results. Furthermore, the Mg concentrations in both samples were closely matched.

4.1.2. XRD results. All the elements encountered were representative of the most common minerals occurring in rocks. Knowledge of mineral composition is more critical in geology and mining than simple elemental analysis. Thus, these elemental results are always supplemented with mineral distribution data derived from laboratory-based XRD analysis. Table 4 shows the results and are compared with the quantitative evaluation of minerals (QEM) scan results. These results they are used further in the discussion section to compare handheld and lab-based equipment capabilities and limitations.

4.1.3. QEM scan results. With advancements in modern optical technology, optical instruments such as QEM have also been utilized to study mineral distribution in thin sections. The results are presented in the form of pictures, and they better represent the mineral distribution in the samples. Table 5 shows the mineral estimation using the QEM scan conducted on thin sections.

From the mineral distribution results from the XRD and QEM scanning instruments, we can observe close matches in most of the results. Given that both instruments use X-ray-based energy dispersive spectroscopy methods, similar results were expected. Although the concentrations of minerals varied, the trend in the concentrations was mostly similar in both results, which is generally sufficient to identify rock types. However, a better representation of the results from the color-based images generated from the QEM scan can be found to be extremely useful for economically important minerals that usually occur in the veins (Fig 6).

4.1.4. Gamma ray results. A handheld gamma-ray tool was also utilized to measure U, Th, and K in the samples. The results are presented as percentages (%) for K owing to its relative abundance in the geological samples and in parts per million (ppm) for U and Th (Table 6). Although these results were compared with the XRF results from other instruments, no suitable

Table 4. *Laboratory X-ray diffraction results (%)*

ID	Rock Type	Dolomite	Calcite	Quartz	Gypsum	Anhydrite	Feldspar	Kaolinite	Chlorite	Hematite	Illite
F1	Granite	0.3	0.2	6.5	0.3	0.4	90.1	0.1	1.1	0	1
F2	Carbonate	98.8	0.3	0	0	0	0.6	0.1	0	0	0.1
F3	Gypsum	18.9	0	0.1	80.2	0.3	0.4	0	0	0	0
F4	Sandstone	0.5	0.3	52.8	1.6	0	2.6	37	3.4	0.1	1.5
F5	Sandstone	0.5	0.2	95.7	0.7	0.1	0.6	1.4	0.2	0.2	0.4
F6	Anhydrite	0.2	0	0.2	98.8	0.1	0.4	0	0	0	0.1
F7	Carbonate	99	0	0.1	0.1	0	0.4	0	0	0.1	0.3
F8	Carbonate	99.1	0	0	0.2	0	0.3	0	0.1	0.1	0.1

Table 5. *Quantitative evaluation of minerals scan mineral results (%)*

ID	Rock Type	Dolomite	Calcite	Quartz	Gypsum/Anhydrite	Feldspar	Kaolinite	Chlorite	Illite	Pores
F1	Granite	0	0	24.49	0	71.28	0	1.14	0	0
F2	Carbonate	61.99	0.11	0.75	0.02	0	0	0.02	0.06	36.83
F3	Gypsum	0	0	0.1	79.12	0	0	0	0	20.77
F4	Sandstone	0	0	62.23	0.01	0	8.26	1.38	0.05	27.48
F5	Sandstone	0	0.02	72.27	0	0	0.79	0.21	0.01	26.43
F6	Anhydrite	0.15	0.03	0.09	95.69	0	0.01	0.02	0.05	3.69
F7	Carbonate	78.19	0	0.55	0.03	0	0	0.01	0.04	21
F8	Carbonate	82.35	0.01	0.27	0.01	0	0	0.05	0.49	16.5

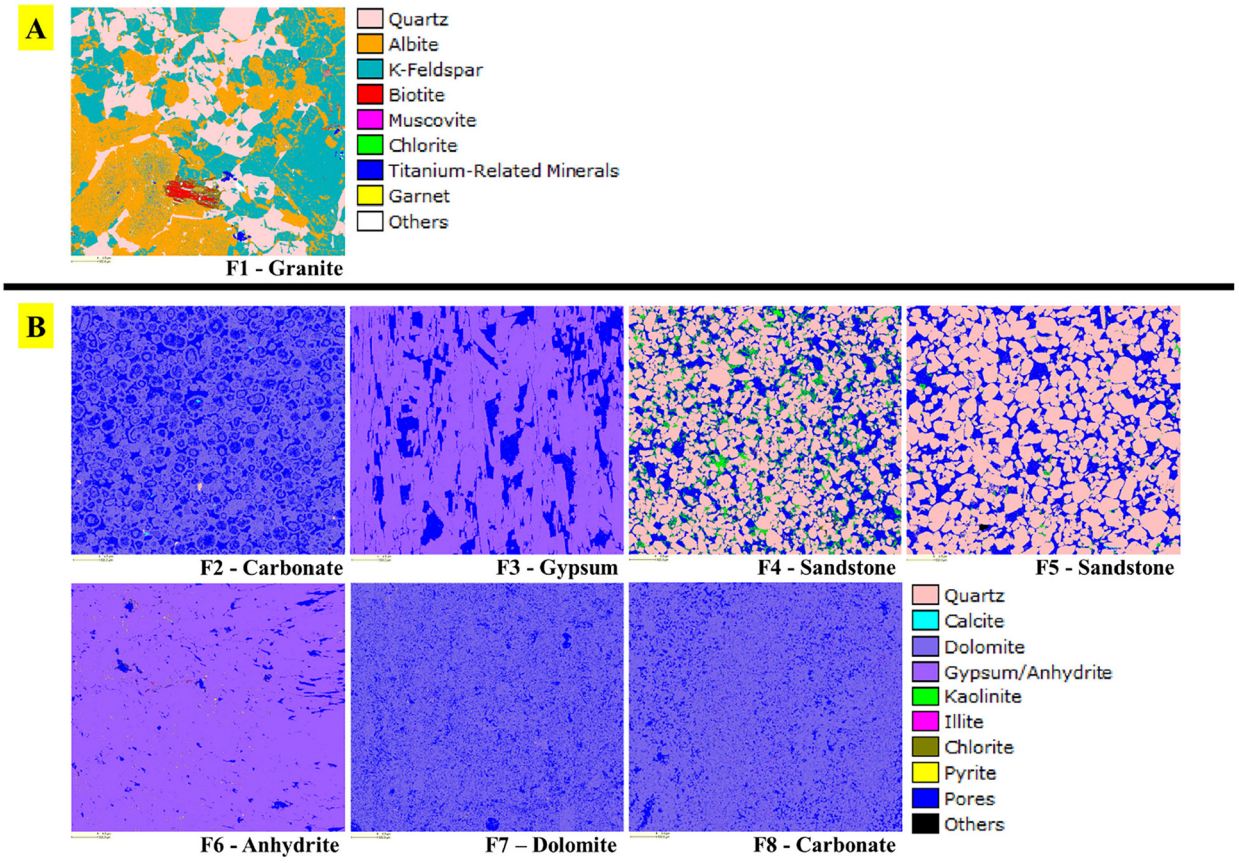

Figure 6. Quantitative evaluation of minerals by scanning electron microscopy images of the samples. F1 follows the legend in (a), whereas F2-8 follow the legend in (b)

Table 6. *Gamma ray data*

ID	Rock Type	K (%)	U (ppm)	Th (ppm)	Dose Rate (nGy/h)
F1	Granite	0.67	1.51	4.20	27.83
F2	Carbonate	0.51	1.36	4.96	26.77
F3	Gypsum	0.74	2.03	4.21	31.65
F4	Sandstone	0.67	0.84	5.38	26.92
F5	Sandstone	0.58	1.52	4.57	27.59
F6	Anhydrite	0.70	0.61	5.69	26.77
F7	Carbonate	0.46	1.98	3.73	26.59
F8	Carbonate	0.57	2.02	4.00	28.86

trend was noted between the K readings, making them unsuitable for comparison. Similarly, U and Th were lower than the detection limits of both handheld and lab-based XRF equipment, rendering readings from gamma-ray tools unusable.

4.2. Petrophysical Results. Table 7 lists the pore spaces present in the samples and their connectivity measured using portable instruments. The porosity results of the samples calculated using QEM Scan analysis and the traditional point-counting technique performed on thin sections are also shown in the table.

These methods use different principles to estimate pore spaces and compare the porosity results. TinyPerm is based on the connectivity of pores, whereas the other two methods estimate the total pore spaces and not their connectivity. Considering that the comparison of porosity with effective porosity (permeability) is a standard practice in reservoir characterization studies, we attempted to compare them. Thus, the results drawn from the Tinyperm were used for comparison only and not for direct porosity-permeability correlation.

For sample F1, a match can be observed in all results. As it is an igneous rock, its porosity and permeability are extremely low. The slightly higher permeability observed in the Tinyperm instrument can be attributed to leakage from the equipment nozzle or the presence of minor fractures in the rock, which are common in igneous rocks. Furthermore, the results from the thin-section petrography scan verified these results, wherein some fractures were noted that represent 3% porosity. Considering that the QEM Scan area is generally extremely small, no porosity was detected in the area scanned from the thin section.

For sandstones (F4 and F5), Tinyperm revealed extremely high porosity, which was confirmed by both the QEM Scan and thin-section petrography results. However, for carbonates (F2, F7, and F8), Tinyperm porosity values were substantially lower than those observed in the QEM and thin-section petrography results. As the carbonates demonstrate considerable dissolution porosity in the form of dissolved carbonate grains. However, this dissolution can also lead to the clogging of pore spaces, occluding the permeability of these rocks. In the case of gypsum (F3) and anhydrite (F6), gypsum shows some porosity owing to its fibrous nature, whereas anhydrite is a massive and very tight rock, showing exceptionally low porosity and permeability values.

5. DISCUSSION

Comparative analysis of geological samples using handheld and laboratory-based geochemical and petrophysical methods showed significant concordance (as expected) and some discrepancies, underscoring the limitations and sensitivity of each analytical methodology. At first glance, the XRF datasets from both instruments seem to be mostly the same, especially for samples rich in silica (Si). For the igneous sample (F1), a close match in the Si levels between the two tools suggests that they could accurately measure the main framework elements. However, the differences in aluminum (Al), iron (Fe), and potassium (K) underscored some systematic differences. Contrastingly, the higher Fe and K levels in the handheld measurements were probably owing to surface heterogeneity, shallow penetration depth, and/or lower spectral resolution.

A similar trend was observed in the sandstone samples (F4 and F5), although the fact that the silica content was not similar in both results. Moreover, the laboratory instrument provided

Table 7. *Tinyperm permeability (darcy) + quantitative evaluation of mineral scan and thin-section porosity (%)*

ID	Sample Type	Tiny perm Permeability (Darcy)	QEM Scan Porosity (%)	Thin Section Porosity (%)
F1	Granite	0.0011	0	3
F2	Carbonate	0.1509	36.83	32.23
F3	Gypsum	0.0146	20.77	3.33
F4	Sandstone	1.4	27.48	37.55
F5	Sandstone	2.8	26.43	35.33
F6	Anhydrite	0.0069	3.69	1.67
F7	Carbonate	0.00057	21	10.67
F8	Carbonate	0.000472	16.5	23.67

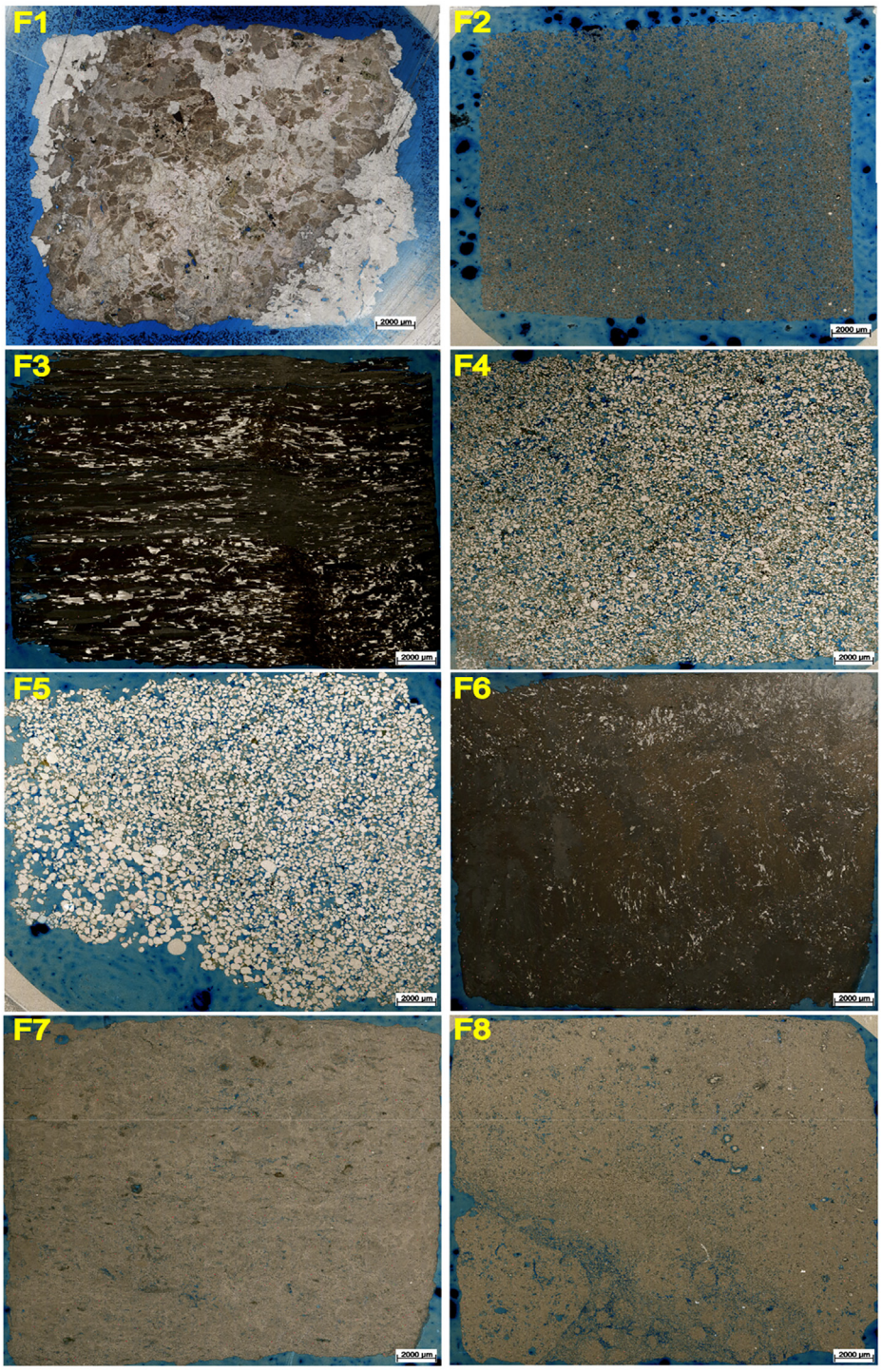

Figure 7. Thin sections scanned using Axio scan. Small red and green dots represent 300 points used in point counting

better results in percentages and overall increasing trend was the same in both methods. However, the differences in aluminum concentrations between the two samples revealed how mineralogical heterogeneities can influence things, particularly the different amounts of feldspars and clay minerals. This indicates that handheld XRF is proficient in detecting predominant elements but may show reduced reliability in precisely quantifying elements associated with secondary or fine-grained mineral phases.

Large differences were observed in the carbonate samples (F2, F7, and F8), where the Ca and Mg concentrations were inversely related between the handheld and laboratory datasets. Laboratory XRF always revealed high Ca levels and low Mg levels. Contrastingly, handheld results revealed lower Ca levels and higher Mg levels. This difference is probably because Ca and Mg behave similarly in the carbonate crystal lattices and can replace each other. Overlapping spectral peaks and matrix effects make it harder to distinguish elements, particularly for handheld

devices with lower spectral resolution. Uneven surfaces and different sample types may worsen these differences. However, any carbonate with >13% Mg can be termed dolomite; therefore, this does not considerably affect the results. The uniform results for gypsum (F3) and anhydrite (F6), particularly concerning S and Mg, suggest that this issue is predominantly confined to carbonate systems rather than sulfate minerals. This corroborates the interpretation that Ca–Mg substitution and spectral overlap are the main sources of analytical inconsistency.

The combination of XRD and QEM Scan analyses provided a mineralogical framework that supported and improved elemental data. Both methods revealed that the mineralogical trends were extremely similar, which means that dominant mineral phases were present in all samples. Although the amounts of minerals differed, the relative amounts were still sufficiently stable for lithological classification. The consistency of each method is attributed to the analytical principles involved. XRD uses crystallographic properties to determine the bulk mineral composition, whereas QEM scans use energy-dispersive spectroscopy on thin sections to create high-resolution spatial maps. The visual output of the QEM scan are another benefit because they clearly reveal the locations of the minerals. This is particularly useful for identifying minerals that are crucial for the economy in small areas, such as veins.

Although gamma-ray measurements were designed to augment the XRF data by quantifying potassium, uranium, and thorium, they exhibited some limitations in this study. The absence of a definitive correlation between potassium values derived from gamma ray and XRF analyses indicates discrepancies in the principles of measurement, calibration, and sensitivity. The uranium and thorium concentrations were too low to be detected by the XRF equipment. Therefore, gamma-ray data could not be utilized for comparison. This reveals that finding trace elements in samples with low levels of radioactivity is challenging, and the importance of using more sensitive methods.

From a petrophysical perspective, a comparison of the porosity and permeability results underscores the necessity of understanding the basic principles of each methodology. The agreement between all methods for the igneous sample (F1) confirmed its low porosity and permeability. The minor differences noted were owing to the microfractures identified in the thin-section analysis, which were not completely captured by the QEM Scan. Contrastingly, sandstone samples (F4 and F5), revealed consistently high porosity across all methods. This means that the pore networks are well-connected and that direct and indirect methods work well for these types of rocks. However, the carbonate samples presented a different trend. The substantially lower permeability values obtained from the TinyPerm instrument compared to the higher porosity values from the QEM Scan and thin-section petrography analyses highlighted the difference between the total pore volume and pore connectivity. Carbonates commonly show secondary porosity, especially dissolution features, which can increase the total pore space while decreasing permeability owing to pore throat blockage or cementation. Finally, the contrasting behaviors of gypsum (F3) and anhydrite (F6) further show the effect of the mineral texture, with the fibrous structure of gypsum allowing some porosity, whereas the dense crystalline nature of anhydrite results in minimal pore development.

The effect of the mineralogy of a rock on its porosity and permeability can be easily observed by comparing the petrophysical and mineralogical results. Granite (F1), an igneous rock formed under high-temperature/pressure conditions, demonstrates a close packing of minerals with almost no porosity. Contrastingly, sandstones (F4, F5), formed mostly on the surface via physical processes. The compaction of these sandstones depends on the depth of burial and diagenetic processes. A lower burial depth indicates lower compaction and less diagenetic alteration, resulting in higher porosity values, as is evident in our samples, where the highest porosity and permeability values were noted in the sandstone samples. Carbonates, however, present a complex case, formed mostly by chemical and biological processes involving extremely fine-grained sediments, and show extremely low inherent porosity. Most of the porosity in carbonates is secondary and is formed either by dissolution or by fracture systems developed during burial and diagenesis. In our carbonate samples (F2, F7, and F8), the effect of dissolution was easily observed in the thin-section images. F2, which dissolved the most, had the highest porosity values. Contrastingly, F7 and F8 showed more compaction and relatively less dissolution (because of their higher dolomite content), leading to relatively lower porosity values. Evaporites, which are also chemically precipitated rocks, show lower initial porosity values and are mostly preserved because of their ductile nature. Although gypsum (F3) revealed higher QEM Scan porosity values, this was mostly attributed to the dissolution effects caused by sample preparation.

6. CONCLUSIONS

This study compared the technical efficiencies of handheld and laboratory-based geochemical and petrophysical measurement tools for various specimens with different lithologies. While handheld instruments provide rapid and reasonably reliable field-based evaluations, laboratory methods remain critical for the precise quantification and detailed mineralogical characterization of rocks. Therefore, the integration of multiple analytical methods, both field- and laboratory-based, is suggested for a comprehensive understanding of geological materials, especially in complex systems such as carbonates, where compositional and structural factors can substantially affect the analytical outcomes.

AFFILIATIONS AND AUTHOR DETAILS

Undergraduate Author

Farah Abdullah Alajmi – *College of Petroleum Engineering & Geosciences, King Fahd University of Petroleum & Minerals, Dhahran 31261, Saudi Arabia*; 0009-0006-5600-6040
Email: s202322710@kfupm.edu.sa

Corresponding Author

Muhammad Hammad Malik – *Research Mentor, Researcher, College of Petroleum Engineering & Geosciences, King Fahd University of Petroleum & Minerals, Dhahran 31261, Saudi Arabia*; 0000-0002-9451-0188
Email: muhammad.malik.1@kfupm.edu.sa

ACKNOWLEDGEMENTS

The authors would like to acknowledge the support provided by the Geosciences Department of the College of Petroleum Engineering and Geosciences as well as Center for Integrated Petroleum Research at King Fahd University of Petroleum and Minerals for providing research and analytical facilities. The authors also extend their appreciation to the technical staff and laboratory team for their assistance with sample preparation and testing. All samples were analyzed using in-house equipment at the Center of Integrated Petroleum Research, KFUPM, Saudi Arabia.

REFERENCES

(1) Lemière, B., 2018. A review of pXRF (field portable X-ray fluorescence) applications for applied geochemistry. J. Geochem. Explor. 188, 350–363. https://doi.org/10.1016/j.gexplo.2018.02.006

(2) Young, K.E., Evans, C.A., Hodges, K.V., Bleacher, J.E., Graff, T.G., 2016. A review of the handheld X-ray fluorescence spectrometer as a tool for field geologic investigations on Earth and in planetary surface exploration. Appl. Geochem. 72, 77–87. https://doi.org/10.1016/j.apgeochem.2016.07.003

(3) Piercey, S.J., Devine, M.C., 2014. Analysis of powdered reference materials and known samples with a benchtop, field portable X-ray fluorescence (pXRF) spectrometer: evaluation of performance and potential applications for exploration lithogeochemistry. Geochem. Explor. Environ. Anal. 14, 139–148. https://doi.org/10.1144/geochem2013-199

(4) Bourke, A., Ross, P.-S., 2016. Portable X-ray fluorescence measurements on exploration drill-cores: comparing performance on unprepared cores and powders for 'whole-rock' analysis. Geochem. Explor. Environ. Anal. 16, 147–157. https://doi.org/10.1144/geochem2014-326

(5) Laperche, V., Lemière, B., 2020. Possible Pitfalls in the Analysis of Minerals and Loose Materials by Portable XRF, and How to Overcome Them. Minerals 11, 33. https://doi.org/10.3390/min11010033

(6) Al-Lehyani, A., Eltom, H.A., Al-Shuhail, A., Abdullah, E., El-Husseiny, A., 2025. Comparative study of laboratory and portable spot permeability measurements in bioturbated carbonate strata. Sci. Rep. 15, 15947. https://doi.org/10.1038/s41598-025-00697-w

(7) Gazley, M.F., Bonnett, L.C., Fisher, L.A., Salama, W., Price, J.H., 2017. A workflow for exploration sampling in regolith-dominated terranes using portable X-ray fluorescence: comparison with laboratory data and a case study. Aust. J. Earth Sci. 64, 903–917. https://doi.org/10.1080/08120099.2017.1367721

(8) Hussain, A., & Al-Ramadan, K. (2022). A core-based XRF scanning workflow for continuous measurement of mineralogical variations in clastic reservoirs. MethodsX, 9, 101928. https://doi.org/10.1016/J.MEX.2022.101928

(9) Hussain, A., Butt, M.N., Olariu, C., Malik, M.H., Koeshidayatullah, A., Amao, A., Al-Ramadan, K., 2022. Unravelling reservoir quality heterogeneity in mixed siliciclastic-carbonate deposits: An example from Miocene Red Sea rift, NW Saudi Arabia. Mar. Pet. Geol. 145, 105850. https://doi.org/10.1016/j.marpetgeo.2022.105850

(10) Malik, M. H., Chan, S. A., Babalola, L. O., Kaminski, M. A., 2022. Optimization of the acetic acid method for microfossil extraction from lithified carbonate rocks: Examples from the Jurassic and Miocene limestones of Saudi Arabia. MethodsX, 9, 101828. https://doi.org/10.1016/j.mex.2022.101828.

(11) Shand, C.A., Wendler, R., 2014. Portable X-ray fluorescence analysis of mineral and organic soils and the influence of organic matter. J. Geochem. Explor. 143, 31–42. https://doi.org/10.1016/j.gexplo.2014.03.005

(12) Gałuszka, A., Migaszewski, Z.M., Namieśnik, J., 2015. Moving your laboratories to the field – Advantages and limitations of the use of field portable instruments in environmental sample analysis. Environ. Res. 140, 593–603. https://doi.org/10.1016/j.envres.2015.05.017

(13) Lima, M., Sanjurjo-Sánchez, J., Alves, C., 2017. Assessment by Portable Gamma Spectrometry of External Gamma Radiation Hazard due to Granitic Materials and Indoor Space Typology. Geosciences 7, 131. https://doi.org/10.3390/geosciences7040131

(14) Sanjurjo-Sánchez, J., Arce Chamorro, C., Alves, C., Sánchez-Pardo, J.C., Blanco-Rotea, R., Costa-García, J.M., 2018. Using in situ gamma ray spectrometry (GRS) exploration of buried archaeological structures: A case study from NW Spain. J. Cult. Herit. 34, 247–254. https://doi.org/10.1016/j.culher.2018.05.004

(15) Bello, A.M., Al-Ramadan, K., Koeshidayatullah, A.I., Amao, A.O., Herlambang, A., Al-Ghamdi, F., Malik, M.H., 2023. Impact of magmatic intrusion on diagenesis of shallow marine sandstones: An example from Qasim Formation, Northwest Saudi Arabia. Front. Earth Sci. 11, 1105547. https://doi.org/10.3389/feart.2023.1105547

(16) Malik, M.H., Hussain, A., Koeshidayatullah, A., Strauss, J.V., Herlambang, A., Bello, A.M., Al-Ramadan, K., 2025. Sedimentary architecture of the ediacaran mixed carbonate-siliciclastic system, NW arabian plate: Regionally extensive marine incursion or syntectonic fault-controlled basin? Precambrian Res. 427, 107872. https://doi.org/10.1016/j.precamres.2025.107872

(17) Amao, A.O., Al-Ramadan, K., Koeshidayatullah, A., 2016. Automated mineralogical methodology to study carbonate grain microstructure: an example from oncoids. Environ. Earth Sci. 75, 666. https://doi.org/10.1007/s12665-016-5492-x

(18) Amao, A.O., Al-Otaibi, B., Al-Ramadan, K., 2022. High-resolution X–ray diffraction datasets: Carbonates. Data Brief 42, 108204. https://doi.org/10.1016/j.dib.2022.108204

(19) Malik, M. H., Al-Yaseri, A., & Al-Ramadan, K. (2026). Evaluating calcite as a catalyst for pyrite-hydrogen reactions and hydrogen sulfide generation. Energy Geoscience, 7(2), 100525. https://doi.org/10.1016/J.ENGEOS.2026.100525